Robust Segmentation and Anatomical Labeling of the Airway Tree from Thoracic CT Scans

Bram van Ginneken, Wouter Baggerman, and Eva M. van Rikxoort

Image Sciences Institute, University Medical Center Utrecht, The Netherlands

Abstract. A method for automatic extraction and labeling of the airway tree from thoracic CT scans is presented and extensively evaluated on 150 scans of clinical dose, low dose and ultra-low dose data, in inspiration and expiration from both relatively healthy and severely ill patients. The method uses adaptive thresholds while growing the airways and it is shown that this strategy leads to a substantial increase in the number, total length and number of correctly labeled airways extracted. From inspiration scans on average 170 branches are found, from expiration scans 59.

1 Introduction

Multi-slice CT scanning technology has revolutionized the in vivo study of the lungs and motivates the need for pulmonary image analysis [1]. Automated extraction and labeling of the bronchial tree from thoracic CT scans is vital to accurately quantify airway morphology which is increasingly used to measure progression and response to treatment for a variety diseases. Another important application is computer-assisted bronchoscopy.

A wide variety of methods have been developed to segment the airways [2,3,4,5,6,7,8,9,10,11]. Some of these include or focus specifically on anatomical labeling of airway segments [2,12,13]. Most methods have been evaluated on a small number of scans. Evaluation on low-dose scans is rare ([14] is an exception), as are application to expiration scans and scans with substantial pathology.

In this work, a method is proposed to segment the complete airway tree. Our approach is based on the generic tree extraction framework outlined in [4,6] and introduces several modifications and new rules for accepting segments. A key contribution is the introduction of a multi-threshold approach to increase robustness. Furthermore, a novel algorithm for anatomical labeling is presented.

Extensive results are presented from 150 scans that include clinical dose, low dose and ultra low-dose, inspiration and expiration scans and data from asymptomatic subjects as well as interstitial lung disease patients with massive pathology.

2 Method

The backbone of our algorithm is an implementation of the framework given in [4,6]. In this section we discuss the initialization, briefly review the framework, describe

our rules for accepting voxels, fronts and segments, introduce the multi-threshold extension of the method and finally describe the anatomical labeling algorithm.

Initialization. The trachea and the lungs are automatically segmented with a method based on [15,16]. Central dark circular regions are searched to find a start point in the trachea, followed by region growing with multiple optimal thresholds to extract the trachea and the lungs. The lung segmentation is used to infer the scan orientation. From the trachea segmentation a seed point is determined in the axial slice that contains the center of gravity of the structure. Only growing in the basal direction is allowed.

Tree segmentation framework. The segments of the bronchial tree are obtained by wavefront propagation. The initial seed point provides the first front. At every iteration, all unprocessed voxels connected to the front that satisfy the *voxel criteria* form the new wavefront. The segment is allowed to keep growing when the front meets the *wavefront criteria*. If the new front consists of multiple parts, a segment is complete and accepted if it complies with the *segment criteria*. To avoid spurious front splittings due to noise, a large 80-connectivity value is used to detect them. New fronts are pushed on a stack and the next front from the stack is propagated. The algorithm terminates when the stack is empty. While the fronts propagate, the centerline or skeleton of the tree and the local segment diameter are computed and this information is used in several of the acceptance criteria. An important difference with [4,6] is that we use region growing to obtain the new front. To avoid diamond- or cuboid-shaped fronts, growing is restricted to within a sphere from the last calculated center point with a diameter slightly larger than the last calculated segment diameter.

Rules for accepting voxels, wavefronts and segments. Voxels are accepted when their density (in Hounsfield Units or HU) is below a threshold t, or (to be less sensitive to noise) the HU value in a $3 \times 3 \times 3$ neighborhood around the voxel is $< t$. For every new front, three checks are applied to the segment grown so far, and if they are violated the entire segment is removed. First, the segment's current radius must be smaller than 1.5 times the minimum radius found in any parent segment. This ensures that diameters of bronchi diminish. When leaking occurs, this rule is typically violated. Second, a front is not allowed to touch any other segment (segments are grown in a breadth first fashion). Third, the length of the segment should not be more than 5 times its radius. This ensures that partly grown segments are accepted before a leakage occurs that could discard a large part of an airway. A completed segment is only accepted if it meets two more requirements: The angle it makes with its parent should be $< 100°$ and the average ratio of radii of two consecutive fronts should not exceed 1.1. The latter check ensures that the segment is not widening, which typically indicates leakage.

Postprocessing. After the bronchial tree has been extracted, several postprocessing steps are performed. First all minor trailing segments (i.e. segments without descendants) are removed. Segments are considered minor if their length is smaller than 3 mm and their volume is below 25 mm^3. Next, the tree structure
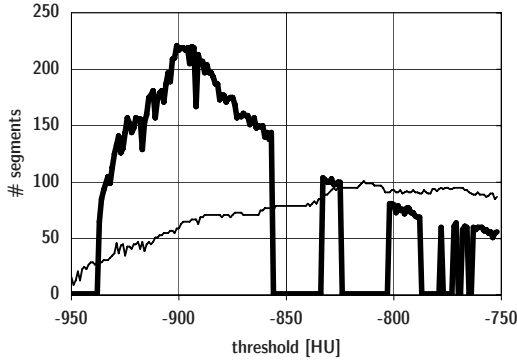
Fig. 1. The total number of segments found in the airway tree as a function of the threshold t for voxel acceptance for two scans. The thick line demonstrates that the results can be sensitive to small changes in t. For both cases, the multi-threshold method found many more segments: 289 and 181 for the thick and thin line, respectively.

is scanned for segments that have exactly one descendant, and these segments are merged. Finally, holes in the segments, primarily caused by noise, are filled. *Adaptive acceptance rules.* We have observed that with these rules for accepting wavefronts and segments, leakage into the parenchyma is virtually impossible to occur, and thus all segments found are true airways. Not all airways are found, however, and in fact it is possible that large parts of the airway tree are missed. Quite often, small changes in the value for the voxel acceptance threshold t, have a profound effect on the number and total length of detected airways. Note that it is not the case that higher values for t automatically lead to more voxels considered airways. Surely, more voxels are accepted when computing a new front when t is increased, but these fronts or these segments may subsequently be rejected by the front and segment acceptance rules. The algorithm thus manifests a complex interplay between the rules at various levels. The effect is illustrated in Fig. 1. This figure also shows that the optimal value for t varies from scan to scan. For most scans, $t = -900$ gives the best results, so this value was used in what we refer to as the single threshold method.

To overcome these limitations and obtain a more robust segmentation that includes as many peripheral airways as possible, we propose to make the process adaptive. Every segment is first grown with a high threshold $t = -750$. If rejected, the segment is regrown with a lower threshold $t + k\Delta t$ with $k = 1, \ldots, 18$ and $\Delta t = -10$. This is referred to as the multi-threshold method. It renders the extraction process adaptive: at every position in the scan the maximum number of airway voxels are selected while the front and segment rules still ensure that no leaking can occur.

Anatomical labeling. After the tree has been segmented, anatomical labels for branches up to the segmental level are automatically assigned. We use 32 distinct labels following the nomenclature from [12]. The fact that trifurcations are usually two consecutive bifurcations lead us to define five small intermediate segments that may or may not be present.

Table 1. Average number and total length (in mm) of all airways per generation, per scan, split over the three databases

| | Database 1 | | | | Database 2 | | | | Database 3 | | | |
| | single | | multi | | single | | multi | | single | | multi | |
gen.	#	length	#	length	#	length	#	length	#	length	#	length
1	2	97	2	99	2	92	2	96	2	88	2	88
2	4	66	4	68	4	64	4	70	4	58	4	59
3	8	102	8	100	7	85	8	103	7	88	8	90
4	14	188	16	214	7	87	13	162	11	141	14	163
5	17	251	27	378	4	50	14	179	15	206	24	298
6	14	193	35	430	2	28	8	85	14	178	32	366
7	10	140	27	330	1	17	5	54	10	130	29	294
8	5	84	18	218	1	9	2	29	7	83	21	208
9	4	62	11	143	0	3	1	10	4	57	15	153
10	2	30	7	92	0	1	0	2	3	35	10	100
11	1	13	4	55	0	0	0	0	2	16	10	61
>11	1	11	5	56	0	0	0	0	2	17	10	69
all	81	1238	166	2183	30	434	59	789	82	1096	174	1949

To assign the labels, the segment labels of 17 trees were manually assigned. The distribution of several segment characteristics were studied, and orientation, average radius, and angle with the parent segment were found most discriminative. Assuming independent normal distributions for these characteristics over the segments, we can measure a probability that a particular label should be assigned to a test segment. To assign the actual label, we look at the probability of the segment conditioned on those of its children and grand children. Labels are assigned in a recursive process, starting at the trachea, which is known from the initial seed point. At every step all unlabeled segments with a labeled parent are considered and the most probable labels are assigned.

3   Experimental Results

Experiments have been performed on three databases, each holding 50 scans from 16-slice scanners or higher, with sub-millimeter near isotropic resolution. Database 1 contains low-dose ($CTDI_{vol} \approx 3$ mGy) scans from a lung cancer screening program from asymptomatic subjects, scanned at full inspiration. Database 2 contains scans from the same subjects, now scanned at ultra-low-dose ($CTDI_{vol} \approx 1$ mGy) at end-expiration. Database 3 consists of scans from patients with interstitial lung disease with severe abnormalities present in the scans, all acquired at full inspiration and with a clinical dose ($CTDI_{vol} \approx 10$ mGy).

We applied both the single and the multi-threshold method to all 150 scans. Table 1 reports the total number of segments found and their length, per generation. Table 2 list for each lobar and segmental branch how often is was detected. Fig. 2 compares the results of the single and multi-threshold method in a

Table 2. For each of the 32 labeled segments in the bronchial tree, the percentages of extraction are listed for each database and for the single threshold method (S) and the multi-threshold method (M)

	Database 1		Database 2		Database 3	
	S	M	S	M	S	M
Trachea	100	100	100	100	100	100
RMB	98	100	100	100	92	96
RUL	96	98	98	100	92	94
RB1	96	98	68	94	82	88
RB2	92	96	72	94	84	86
RB3	94	98	80	96	86	88
BronInt	96	98	98	100	92	94
RB4+5	96	98	86	98	92	94
RB4	74	96	58	88	74	90
RB5	74	96	58	88	74	90
RB6	96	98	86	98	92	94
RLL7	96	98	72	98	82	92
RB7	94	98	62	94	80	88
RLL	94	98	62	94	80	88
RB8	84	98	34	80	62	78
RB9	84	96	40	80	58	80
RB10	84	98	36	80	60	78
LMB	98	100	100	100	92	96
LUL	96	100	94	98	92	92
LB1+2	92	98	76	96	82	92
LB1	82	96	54	88	68	88
LB2	82	96	54	88	68	88
LB3	94	98	40	86	86	88
LB4+5	94	98	90	98	84	90
LB4	80	96	42	74	74	88
LB5	80	96	42	74	74	88
LLB6	96	100	94	98	92	92
LB6	96	98	74	96	84	90
LLB	96	98	74	96	84	90
LB8	88	98	40	82	76	88
LB9	92	98	44	88	76	88
LB10	88	98	38	84	70	86
Overall average	91	98	68	92	81	90

scatterplot. Fig. 3 shows results for Database 1 (low-dose inspiration) versus the most challenging data used in this study, Database 2 (ultra-low dose expiration).

We have evaluated the accuracy of the labeling by asking two trained human observers to click points in each of the 32 segments. In a preliminary study on 36 scans we found that for the branches detected by the multi-threshold algorithm (98, 92 and 90%, for the three databases, respectively) 90% were correctly labeled. Most errors were caused by anatomical variations in the airway trees.
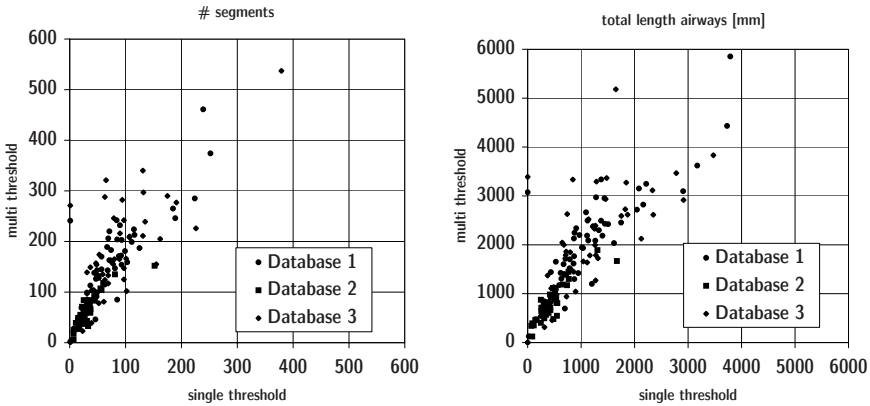
Fig. 2. Scatterplots showing number of segments (left) and total length of all airways in mm (right) found with the single and multi-threshold method. Each point represents one scan.
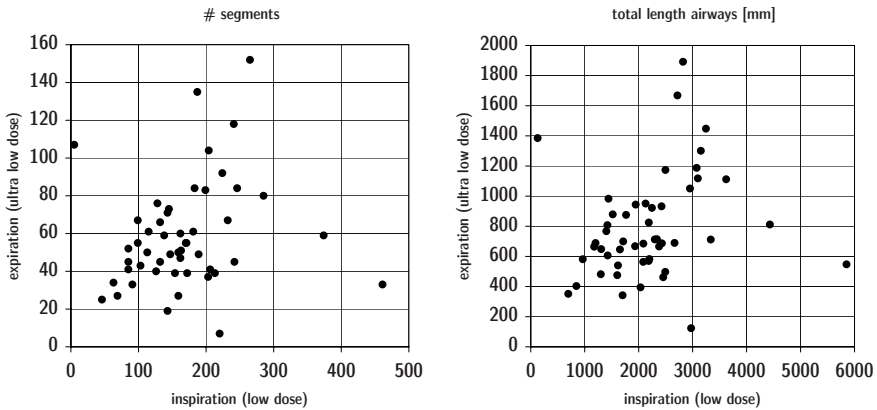

Fig. 3. Scatterplots showing number of segments (left) and total length of all airways in mm (right) found for the 50 scans in Database 1 (low dose, inspiration scans of asymptomatic subjects) versus the 50 scans in Database 2 (same subjects, scanned with ultra low dose in expiration). Each point represents one scan. Note the different scales on horizontal and vertical axis.

4   Discussion and Conclusion

The multi-threshold method effectively uses different HU thresholds for different parts of the bronchial tree. This appears very effective to avoid leakage, and thus early termination of the growth process, which we believe to be the main limitation of the single threshold strategy and previous methods that follow this approach [4,6,14]. Those methods already substantially outperform methods that do not employ the higher level rules at segmental level, like explosion control

region growing. An average number of 170 airways detected in inspiration scans is impressive compared to results reported in other studies. Table 2 shows that the multi-threshold method is capable of extracting the bronchial tree up to segmental level quite robustly, and that its results are substantially better than those of the single threshold method. Both methods produce, by design, almost no false positive findings (incorrect branches). They are also fast, even the multi-threshold growing process requires only around 10 seconds on a single-core PC. The labeling takes less than two seconds.

A limitation of using variable thresholds is that the airway diameter estimation may not be consistent throughout the tree. We believe the current system should be followed by an additional step in which the airway lumen and wall are precisely determined.

In all scans we have inspected, there were very small peripheral bronchi present that were not extracted. A specific search for more distal airways and a mechanism to connect these to the tree [7,10] might improve performance even more. Note that such schemes require vastly more computation time. Another useful extension would be to use more elaborate rules for accepting voxels, fronts and segments, based on more complex image information and statistical analysis, as was recently proposed in [11].

The evaluation of the anatomical labeling is not based on the entire test set and thus preliminary. The accuracy of the procedure could be improved if the possibility of identifying the main anatomical variations in the airway tree up to segmental level were included in the labeling algorithm. Nevertheless it is clear that the majority of labels assigned by our method is correct.

Comparison of the results from Database 1 and 2 shows that the extraction of airways from expiration scans is substantially more difficult, but still generally feasible for the first few generations of the airway tree. The minor differences between Database 1 and 3 show that the proposed method is largely robust to pathology. It is also noteworthy that the total amount and length of airways extracted varies strongly from scan to scan. This makes it clear that comparing results from different methods obtained on different scans is tricky. It would be very useful to compare the different approaches on a single common database.

In conclusion, we have presented a fast, fully automatic method to extract the bronchial tree far into the periphery of the lungs and in addition label the most important branches. By locally adapting the threshold for accepting voxels as being airway, the algorithm is able to grow into airways with thin walls or absent walls at bifurcations, without leaking into the lung parenchyma. Extensive experiments have demonstrated that the method is robust and effective in finding a large number of airways up to ten generations or more.

References

1. Sluimer, I.C., Schilham, A., Prokop, M., van Ginneken, B.: Computer analysis of computed tomography scans of the lung: a survey. IEEE Trans. Med. Im. 25(4), 385–405 (2006)

2. Mori, K., Hasegawa, J., Suenaga, Y., Toriwaki, J.: Automated anatomical labeling of the bronchial branch and its application to the virtual bronchoscopy system. IEEE Trans. Med. Im. 19(2), 103–114 (2000)
3. Swift, R.D., Kiraly, A.P., Sherbondy, A.J., Austin, A.L., Hoffman, E.A., McLennan, G., Higgins, W.E.: Automatic axis generation for virtual bronchoscopic assessment of major airway obstructions. Comp. Med. Imag. & Graph 26, 103–118 (2002)
4. Schlathölter, T., Lorenz, C., Carlsen, I.C., Renisch, S., Deschamps, T.: Simultaneous segmentation and tree reconstruction of the airways for virtual bronchoscopy. In: Proc. SPIE, vol. 4684, pp. 103–113 (2002)
5. Kiraly, A.P., Helferty, J.P., Hoffman, E.A., McLennan, G., Higgins, W.E.: Three-dimensional path planning for virtual bronchoscopy. IEEE Trans Med. Im. 23(11), 1365–1379 (2004)
6. Bülow, T., Lorenz, C., Renisch, S.: A general framework for tree segmentation and reconstruction from medical volume data. In: Barillot, C., Haynor, D.R., Hellier, P. (eds.) MICCAI 2004. LNCS, vol. 3216, pp. 533–540. Springer, Heidelberg (2004)
7. Fetita, C.I., Prêteux, F., Beigelman-Aubry, C., Grenier, P.: Pulmonary airways: 3-D reconstruction from multislice CT and clinical investigation. IEEE Trans. Med. Im. 23(11), 1353–1364 (2004)
8. Tschirren, J., Hoffman, E.A., McLennan, G., Sonka, M.: Intrathoracic airway trees: segmentation and airway morphology analysis from low-dose CT scans. IEEE Trans. Med. Im. 24(12), 1529–1539 (2005)
9. Palágyi, K., Tschirren, J., Hoffman, E.A., Sonka, M.: Quantitative analysis of pulmonary airway tree structures. Comput. Biol. Med. 36(9), 974–996 (2006)
10. Higgins, W.E., Graham, M.W., Gibbs, J.D.: Robust system for human airway tree segmentation. In: Proc. SPIE, vol. 6914 (2008)
11. Lo, P., de Bruijne, M.: Voxel classification-based airway tree segmentation. In: Proc. SPIE, vol. 6914 (2008)
12. Tschirren, J., McLennan, G., Palágyi, K., Hoffman, E.A., Sonka, M.: Matching and anatomical labeling of human airway tree. IEEE Trans. Med. Im. 24, 1540–1547 (2005)
13. Bülow, T., Lorenz, C., Wiemker, R., Honko, J.: Point based methods for automatic bronchial tree matching and labeling. In: Proc. SPIE, vol. 6143 (2006)
14. Wiemker, R., Ekin, A., Opfer, R., Bülow, T., Rogalla, P.: Unsupervised extraction and quantification of the bronchial tree on ultra-low-dose vs. standard-dose CT. In: Proc. SPIE, vol. 6143 (2006)
15. Hu, S., Hoffman, E.A., Reinhardt, J.M.: Automatic lung segmentation for accurate quantitation of volumetric X-ray CT images. IEEE Trans. Med. Im. 20(6), 490–498 (2001)
16. Sluimer, I.C., Prokop, M., van Ginneken, B.: Towards automated segmentation of the pathological lung in CT. IEEE Trans. Med. Im. 24(8), 1025–1038 (2005)